Tellus (1981), *33*, 301–312

Frontal jump conditions for models of shallow, buoyant surface layer hydrodynamics

By RICHARD W. GARVINE, *College of Marine Studies, University of Delaware, Newark, DE 19711, U.S.A.*

(Manuscript received June 10; in final form September 25, 1980)

ABSTRACT

Moving frontal regions are often observed in coastal and inland waters when a buoyant surface layer is present. Examples of such phenomena are moving fronts behind which the spreading of buoyant surface plumes occur and the passage of thermocline surges in lakes. An approach to modeling the hydrodynamics of shallow, buoyant surface layers is suggested which partitions the flow field into a frontal region where dissipative effects are important and an internal wave region where they are not. This approach treats the frontal region as a horizontal discontinuity described by appropriate jump conditions and the wave region by the nonlinear, long internal wave equations. Frontal jump conditions are derived for use in such a model when applied to small-scale flows where earth rotation has a negligible effect. These conditions account for the transport of mass and momentum across the interface with the underlying fluid. They are also applicable to flows where the depth of the buoyant upper layer vanishes on the upstream side of the front. They thus represent an extension of the classical jump conditions associated with an internal bore or hydraulic jump. To illustrate their use in conjunction with the nonlinear internal wave equations, a problem is solved representing the sudden release of a shallow, buoyant upper layer into an unbounded domain. For zero interfacial transport the results are identical to the classical description of the analogous single layer problem posed by the sudden breaking of a dam. For nonzero transport, however, new features of the flow arise.

1. Introduction

In coastal and inland waters a shallow, buoyant upper layer is often found overlying heavier water of substantially greater depth. Two prominent examples are surface plumes of buoyant water originating from a nearby source and the surface layer above the seasonal thermocline in lakes. In both these phenomena, moving frontal regions are often found where the upper layer depth changes rapidly or where the upper layer as a whole spreads outward following a front as it overruns the heavier, ambient water. The purpose of this paper is to derive suitable jump conditions that relate the flow properties on either side of the front to each other and to flow parameters. The role of these jump conditions is then illustrated by the solution of a simple problem representing the sudden release of a pool of buoyant fluid into an open domain. To provide the background for the derivation, I review next the principal known properties and modeling concepts related to plumes and lake thermoclines.

Plumes of buoyant surface water are common features of coastal and inland waters. Their presence is revealed even by the casual observation of such surface properties as changes in color and turbidity, trapped detritus along lines of convergence, and sea state changes. There are a variety of known mechanisms that generate such buoyant plumes. Particular examples are the discharge of fresh or brackish water by rivers, estuaries, or bays into coastal sea water and the discharge of heated water from power plants into lakes, rivers, or the ocean. Of naturally occurring plumes those most studied have been river plumes. Particular examples are the plumes of the Amazon (Ryther, Menzel and Corwin, 1967), the Mississippi (Wright

0040-2826/81/030301-12$02.50/0 © 1981 Munksgaard, Copenhagen

and Coleman, 1971), the Po (Grancini and Cescon, 1973) and the Connecticut (Garvine, 1974a, 1977). The nature of power plant plumes has been documented by Scarpace and Green (1973).

Given our current knowledge, it is useful to divide buoyant plumes into three contiguous spacial fields, here termed the source, near, and far fields. The source field is that in the immediate vicinity of the source of buoyant water, such as the mouth of a river. The near field is where the bulk of the mixing or dilution of buoyant water occurs. Usually its outer boundary is marked by a sharp frontal region. Beyond lies the far field where the final blending of source water with the ambient water occurs. This region is generally diffuse in character and lacks sharp definition.

Frontal features are generally associated with the near fields. In the near field the flow dynamics are dominated by gravitational spreading of a thin layer of buoyant fluid over the heavier ambient fluid. The leading edge of the spreading motion is a frontal region where the horizontal property gradients are largest and where most of the mixing action is concentrated. For river plumes the horizontal extent of the frontal region is about 100 m (Garvine and Monk, 1974). Over the remainder of the near field properties change slowly in space and the vertical stratification is very high. The near field has thus two disparate horizontal length scales, the frontal zone scale and that of the near field as a whole. The near field is inherently time dependent, since its frontal boundary propagates with respect to the ambient fluid at a speed of the order of the phase speed of a long internal wave on the interface beneath the plume (Garvine, 1977).

Most existing plume near field models have a conceptual frame based on the dynamics of the steady-state discharge of a turbulent jet into quiescent ambient water. One of the earliest of these was the analytical study of Takano (1954). Stefan and Vaidyaraman (1972) employed elaborate interfacial friction and mass entrainment parametric forms in a steady state, numerical model. Property variations across the plume were assumed to follow a Gaussian distribution and frontal boundaries were not treated. Stolzenbach and Harleman (1973) developed a similar model.

A model of buoyant plumes of quite different character has been published by Kao, Park and Pao (1977, 1978). Using a finite difference numerical method, they generated solutions of the complete, time-dependent Navier-Stokes equations for a two-dimensional (planar) discharge at a coast into still, ambient water. Solutions showed good agreement with the field data of Garvine and Monk (1974) for the frontal zone structure at the leading edge of the spreading discharge. Between the front and the source the horizontal flow gradients were far lower and the mixing action much reduced. The motion there was suggestive of inviscid, long internal wave dynamics.

Studies of the thermocline motion in lakes have also revealed the frequent occurrence of frontal motion. Hunkins and Fliegel (1973) observed the propagation of large amplitude internal surges as oscillations of the thermocline in Seneca Lake, New York. They sought to explain their observations by applying the inviscid, nonlinear internal wave equations for a homogeneous, shallow upper layer. Many of the oscillatory features they observed could be explained from solutions of the Korteweg–deVries equation called solitons. The inviscid dynamics of the solitons could not explain the net deepening of the interface after passage of a surge which they observed, but they noted that inclusion of internal friction or dissipative effects in the nonlinear wave dynamics could model this behavior. In a related paper Simons (1978) sought to explain the dynamics of propagating thermocline surges or fronts observed as responses to wind stress events in Lake Ontario. He also idealized the stratification with a homogeneous, shallow upper layer and addressed the dynamics using the inviscid, nonlinear wave equations. Sample calculations showed the wave steepening influence of the nonlinear terms which led ultimately to the formation of a front on the interface in the form of an internal bore. While his inviscid analysis could not account for the effect of friction and mass entrainment at the interface, Simons did find that his model reproduced many of the observed characteristics of a particular event with respect to both the motion of the thermocline and the associated currents.

The observations and model studies of buoyant plumes and thermocline motion suggest that a simplified model of the dynamics of shallow, buoyant surface layers is possible. The principal feature of this model is the partitioning of the upper layer flow field into two domains, a frontal domain where dissipative effects are concentrated and

horizontal gradients are very high, and an internal wave domain where they are low. The model would treat the frontal domain as a moving discontinuity across which flow properties were related by appropriate jump conditions. The internal wave domain would be determined by using the nonlinear, long, internal wave equations for a shallow upper layer whose solutions would be found subject to matching with the jump conditions at the frontal boundary (or boundaries). This concept, in fact, is not new, but has been used extensively for the treatment of the analogous problem of shallow, homogeneous single layer flows which include bores or hydraulic jumps (Stoker, 1957, Chapter 10). An advantage of such a simplified model is that it would enable one to solve horizontally one- and two-dimensional, time-dependent flows with greatly reduced analytic or numerical complexity, while retaining the essential physical properties for a variety of applications.

A necessary preliminary to such an approach, then, is the development of suitable frontal jump conditions. These should incorporate the important effects of mass and momentum exchange across the interface with the lower layer, complications which are absent in the single layer problem. In addition, they should remain valid for fronts propagating into regions where no upper layer is present, since in many instances buoyant plumes behave in this way.

These jump conditions are derived in the next section for application to small-scale fronts where earth rotation has a negligible effect. The method used in the derivation is conceptually related to an earlier paper (Garvine, 1974b, hereafter referred to as G74) in which I developed a hydrodynamic model of a small-scale front by using an integral method. The jump conditions derived here may be viewed as a simplification or condensation of the results of that model, as well as its generalization to include a finite interface depth upstream of the front. Alternatively, the jump conditions may be viewed as an extension of the classical bore jump conditions (Stoker, 1957, Chapter 10, Section 6) to include exchange of mass and momentum between two fluid layers and to include the limiting case of vanishing upper layer thickness upstream, analogous to the propagation of a bore down a dry bed.

2. Derivation of the frontal jump conditions

The physical restrictions that apply to the derivation are as follows. The fluid is stratified such that lighter fluid overlies a heavier, ambient fluid of uniform density ρ; however, the density difference will be small so that the Boussinesq approximation may be used. The interface with the ambient fluid is at a variable depth $z = -D$ (see Fig. 1) which is everywhere much smaller than the characteristic water depth h. Earth rotation is neglected; thus, the jump conditions will apply only

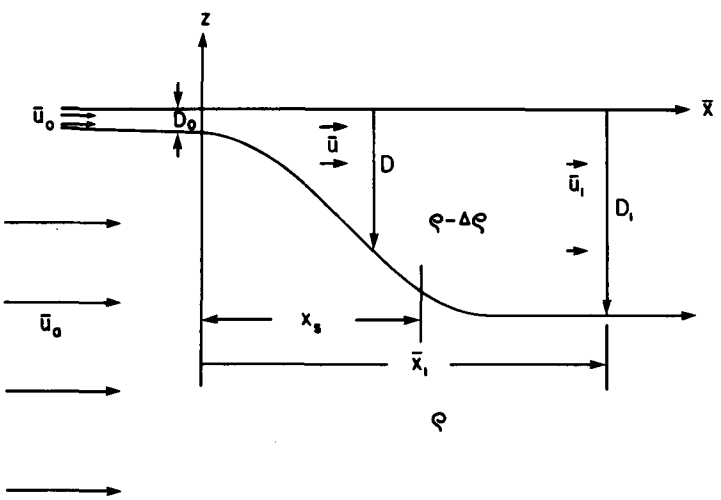

Fig. 1. Schematic diagram of the frontal zone. The interface is at the depth $z = -D$.

to fronts that are sufficiently small in scale. Wind stress is neglected. The vertical momentum balance is assumed to be everywhere hydrostatic. There is no fluid motion in the direction locally parallel to the front. For convenience, above the interface the density will be taken as uniform at $\rho - \Delta\rho$ (with $\Delta\rho/\rho \ll 1$) and the vertical shear of the horizontal velocity there will be neglected (see Fig. 1); these latter two restrictions are not essential, however, and could be removed by using the vertical integral method of G74. Consistent with the second of these, the vertical shear of the ambient fluid will also be neglected. Since this fluid is deep, its horizontal velocity $\bar{u}_a$ is nearly uniform in the horizontal as well. For the special case where the ambient fluid is at rest relative to the earth, $\bar{u}_a$ will simply be the frontal propagation speed.

The coordinates $\bar{x}$, z (Fig. 1) are moving with the front such that the origin lies at the free surface just upstream of where the interface begins to descend from its upstream depth D_0. Downstream at $\bar{x} = \bar{x}_1$ (the overbar denotes a property measured from the moving coordinates) the interface has reached its downstream asymptotic value D_1. The horizontal length scale of the frontal zone is denoted x_s and indicates the extent over which most of the interfacial depth change occurs. Fig. 1 is drawn with considerable vertical exaggeration; in nature, frontal zone interfacial slopes are typically 10^{-2} (Garvine and Monk, 1974) so that x_s will be much larger than $D_1 - D_0$.

The jump conditions may be derived by first integrating the governing equations vertically over the upper layer from $z = -D$ to 0 and then integrating the results over $\bar{x}$ from 0 to $\bar{x}_1$. The vertically integrated continuity equation may be written (G74) as

$$\frac{d}{d\bar{x}}(\bar{u}\mathrm{D}) = q_e(\bar{x}) \tag{1}$$

where q_e is the vertical velocity of mass entrainment at the interface by turbulent motion. For two immiscible fluid layers or for laminar motion, $q_e = 0$; however, for the strongly turbulent motion characteristic of frontal zones, significant entrainment occurs (Garvine and Monk, 1974). After integrating (1) over $\bar{x}$ we have

$$\bar{u}_1 D_1 - \bar{u}_0 D_0 = \int_0^{\bar{x}_1} q_e(\bar{x})d\bar{x} \tag{2}$$

The horizontal ($\bar{x}$) momentum equation, after vertical integration, is

$$\frac{d}{d\bar{x}}(\bar{u}^2 D) - q_e \bar{u}_a = -g' D \frac{dD}{d\bar{x}} + \frac{\tau}{\rho} \tag{3}$$

Here $g' \equiv (\Delta\rho/\rho)g$ (where g is the acceleration of gravity) is the reduced gravity and τ is the shear stress applied to the upper layer at the interface by the relative motion of the ambient fluid. The first term on the left of (3) represents the advection of momentum and the second the flux of momentum by mass entrainment. For this flux the horizontal velocity of a fluid parcel at the interface is taken for simplicity as $\bar{u}_a$, since, in general, $\bar{u}_a$ will be much larger than typical speeds in the upper layer relative to the moving coordinates. The first term on the right represents the vertically integrated horizontal pressure gradient as determined from hydrostatic balance and from the requirement that below the interface the horizontal pressure gradient must vanish (G74). After integrating (3) over $\bar{x}$ we have

$$\bar{u}_1^2 D_1 - \bar{u}_0^2 D_0 + \frac{g'}{2}(D_1^2 - D_0^2) = \int_0^{\bar{x}_1} \left(q_e \bar{u}_a + \frac{\tau}{\rho}\right) d\bar{x} \tag{4}$$

Note that in the absence of both mass and momentum transport across the interface (q_e and τ equal to zero) the right sides of (2) and (4) vanish. The resulting equations are then the same as those for an internal bore and are directly analogous to those for an external bore given by Stoker (1957, p. 318). They are then also related to the results of Yih and Guha (1955), Mehrotra (1973) and Mehrotra and Kelly (1973). They analyzed the internal hydraulic jumps that could exist in flows of two homogeneous fluid layers of different densities. Their treatments differed from the present one in that they neglected interfacial mass and momentum transport but included flows where the two layer depths were comparable. None considered cases where either fluid layer depth could vanish on either side of the jump.

To proceed, parametric forms relating q_e and τ to bulk flow properties are needed. Standard empirical forms are

$$q_e = E\bar{u}_a$$

and

$$\tau = C_f \rho \bar{u}_a^2$$

where E is the interfacial mass entrainment coefficient and C_f the interfacial shear stress coefficient. Here $\bar{u}_a$ has been used to represent the bulk shear velocity across the interface. Following G74, the following forms for E and C_f are adopted:

$$E = S_e a T(\bar{x}) \tag{5a}$$

$$C_f = d a T(\bar{x}) \tag{5b}$$

where S_e denotes the sign of the entrainment velocity ($S_e = 1$ for upward and -1 for downward entrainment), a is the maximum magnitude of E in the frontal zone (typically 10^{-3} to 10^{-2}), $d \equiv C_f/|E|$ is a positive, order one constant and $T(\bar{x})$ is a non-negative distribution function for E and C_f in the frontal zone whose maximum is unity. As discussed in G74 and Garvine (1979) turbulence production near the interface in the frontal zone should arise primarily from the local breaking of internal waves. Laboratory experimental evidence for this is clearly presented by Britter and Simpson (1978) for the analogous problem of a gravity current where heavier fluid moves along the bottom of a flume containing lighter ambient fluid. The turbulence generated by the breaking motion in the frontal zone (or head wave, as it is termed for a gravity current) diminishes to low background levels in the region downstream where the interface is nearly level. To model this behavior I have chosen T as

$$T(\bar{x}) = \exp(-\bar{x}/\beta x_s) \tag{6}$$

where β is an order one, positive constant. Thus, βx_s is the decay scale for interfacial turbulence in the frontal zone.

The frontal zone scale x_s may be written as

$$x_s = (D_1 - D_0)/a \tag{7}$$

This is equivalent to stating that the frontal zone interfacial slope is of the order of $dD/d\bar{x} \sim a$, as shown by the scaling analysis of G74.

After using (5)–(7) the integrals over q_e and τ in (2) and (4) may be evaluated. After defining $\bar{x}_1$ as the location of the downstream frontal zone limit where $T(\bar{x}_1) \ll 1$, (2) and (4) may be written

$$\bar{u}_1 D_1 - \bar{u}_0 D_0 = S_e \beta \bar{u}_a (D_1 - D_0) \tag{8}$$

$$\bar{u}_1^2 D_1 - \bar{u}_0^2 D_0 + \frac{g'}{2}(D_1^2 - D_0^2) = (S_e + d)\beta \bar{u}_a^2 (D_1 - D_0) \tag{9}$$

Equations (8) and (9) admit the trivial solution, $D_1 = D_0$ and $\bar{u}_1 = \bar{u}_0$, as one would expect. They also reduce to the internal bore solution for the limit $\beta \to 0$, since then the extent of the frontal zone over which appreciable interfacial mass entrainment and friction are present would be negligible, as (6) shows.

By combining (8) and (9) so as to eliminate $\bar{u}_1$ one may readily obtain a single equation for D_1 which contains the given variables $\bar{u}_0$ and D_0. This is most conveniently developed by using the following dimensionless quantities:

$$\delta \equiv D_1/D_0$$

$$F_{00} \equiv \bar{u}_0/c_0$$

$$F_{a0} \equiv \bar{u}_a/c_0$$

where $c_0 \equiv (g' D_0)^{1/2}$, the long, linear internal wave phase speed upstream. The symbol F here, as in the remainder of the paper, denotes an internal Froude number. Its first subscript indicates the region for the fluid speed that forms the numerator and the second the region for the phase speed. There are three regions in all, that of the upper layer upstream of the frontal zone (subscript "0"), the upper layer downstream (subscript "1"), and the ambient fluid (subscript "a"). The equation for δ then appears as:

$$\delta^3 + 2\beta(\beta - S_e - d)F_{a0}^2 \delta^2 + [4S_e \beta F_{00} F_{a0} + 2\beta(d + S_e)F_{a0}^2 - 4\beta^2 F_{a0}^2 - 2F_{00}^2 - 1]\delta + 2(F_{00} - S_e \beta F_{a0})^2 = 0 \tag{10}$$

This cubic in δ may be readily factored since we know that $\delta = 1$ must be a root, corresponding to the trivial solution of (8) and (9). After factoring (10) and finding the roots of the remaining quadratic we have

$$\delta = (\pm\sqrt{B^2 + 4C} - B)/2$$

where

$$B \equiv 1 - 2\beta(d + S_e - \beta)F_{a0}^2$$

and

$$C \equiv 2(F_{00} - S_e \beta F_{a0})^2$$

Since $C > 0$, both roots for δ are real and will have opposite signs. We reject the negative root,

since it has no physical meaning. Thus, the solution for δ is

$$\delta = (\sqrt{B^2 + 4C} - B)/2 \tag{11}$$

With δ (or D_1) determined, $\tilde{u}_1$ may be readily computed from (8) to complete the frontal jump conditions. With $\tilde{u}_1$ incorporated into the Froude number $F_{10} \equiv \tilde{u}_1/c_0$, one finds

$$F_{10} = F_{00}\,\delta^{-1} + S_e \beta F_{a0}(1 - \delta^{-1}) \tag{12}$$

The frontal jump conditions (11) and (12) depend upon five dimensionless parameters, two Froude numbers, F_{00} and F_{a0}, and three properties of the interfacial transport processes, S_e, β and d.

Two limiting cases are of particular interest, the internal bore limit ($\beta \to 0$), and the surface front limit for which the upstream upper layer thickness D_0 vanishes ($F_{a0} \to \infty$). For the internal bore, the limiting form for δ is simply

$$\lim_{\beta \to 0} \delta = (\sqrt{1 + 8F_{00}^2} - 1)/2 \tag{13}$$

This result is a direct analogue to that given by Stoker (1957, p. 336) for the external bore as well as to that given by Yih and Guha (1955, eq. (17)) for a two-layer, internal hydraulic jump where the lower layer is at rest. Only one parameter remains. For the surface front limit, $\delta \to \infty$, since $D_0 \to 0$. Then it is more meaningful to express the result in terms of another Froude number,

$$F_{a1} \equiv \tilde{u}_a/c_1$$

where $c_1^2 \equiv g' D_1$. Since $\delta = (F_{a0}/F_{a1})^2$ from the definitions, the limiting form of (11) may be found as

$$\lim_{F_{a0} \to \infty} F_{a1} = [2\beta(d - \beta + S_e)]^{-1/2} \tag{14}$$

From (14) it is clear that the surface front limit requires non-vanishing interfacial transport ($\beta > 0$) if the frontal propagation speed relative to the ambient fluid (or $\tilde{u}_a$) is to be finite. The analogous hydraulic problem for the motion of a single layer is that of a fluid surge behind a front or head wave propagating over a dry bed. Since β and d will be in general of order one, F_{a1}, in this limit should be also. This result is expected based on previous work. Using an inviscid analysis for the analogous problem of a shallow density current, von Kármán (1940) found $F_{a1} = 2^{1/2}$. Kao, Park and Pao (1978) found $F_{a1} \simeq 1.0$ from their numerical solutions for the present limiting case for a wide range of flow parameters such as Reynolds number. In G74 I compared the integral model results to field observations (Garvine and Monk, 1974) for which $F_{a1} \simeq 1.3$. The integral model parameters correspond to $\beta = 0.1$, $S_e = -1$ and $d = 5.5$. Using these in (13) gives $F_{a1} \simeq 1.1$. Consequently, the frontal jump conditions, as given by (11) and (12) give satisfactory results for both the internal bore and the surface front limits. Such agreement lends support to their use for intermediate conditions (when both interfacial transport and a subsurface front exist), even in the absence of confirming observational or laboratory data.

3. Sudden release of a buoyant fluid layer

To illustrate the incorporation of the new frontal jump conditions in the analysis and the physics of a flow I solve in this section the problem posed by the sudden release of a shallow, buoyant upper layer of fluid from a semi-infinite pool into an adjacent unbounded domain. A sketch of the initial upper layer configuration in a vertical section appears in Fig. 2. Initially all fluid is at rest with respect to the fixed coordinates x, z. A membrane separates the upper layer into two regions, the buoyant pool of depth D_p and an adjacent region where $x > 0$ of depth $D_0 < D_p$. Both regions have the same reduced gravity g'. At time $t = 0$ the membrane is instantly removed. Since no variations are then present in the direction normal to the x, z plane and since earth rotation is negligible, the resulting motion will remain independent of the normal direction. The ambient fluid will remain at rest, except in a thin shear layer near the interface, since it is much deeper than D_p. The analogous single-layer problem is the classical one of the sudden breaking of a dam. Stoker (1957, pp. 333–341) has given its

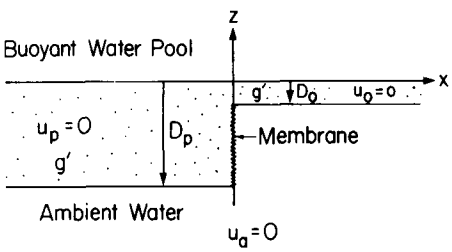

Fig. 2. Initial configuration in a vertical plane of the upper layer for the sudden release problem.

solution using the jump conditions for an external bore corresponding to $\beta = 0$ in Section 2.

Initially the flow will be highly complicated as the initial depth discontinuity provokes breaking of the interface. However, after a short time a front will form which advances toward the right and which has a time averaged configuration (with respect to turbulent fluctuations) that is time invariant when viewed from coordinates traveling with it. The time scale for establishment of this mean configuration will be the turbulent kinetic energy dissipation time for the frontal zone. For small-scale fronts this time is of the order x_s/c_p where $c_p^2 \equiv g' D_p$, or roughly the time for the front to advance by its own horizontal length scale. A similar frontal establishment time is evident in the numerical results of Kao, Park and Pao (1977, Fig. 1a).

In this analysis the upper layer flow after frontal establishment will be analyzed by partitioning it into two major zones, the frontal zone and the remainder of the disturbed upper layer. The frontal zone will be treated as a discontinuity, that is, one whose horizontal scale x_s is small compared to $c_p t$, the scale of the disturbed upper layer. This is tantamount to treating the flow for times large compared to the establishment time. The frontal zone dynamics will be described only through the frontal jump conditions. The dynamics of the remainder of the disturbed upper layer will be described by the nonlinear, inviscid, long internal wave equations; hence this zone will be termed the wave zone. The wave description assumes that interfacial transport of mass and momentum is negligible everywhere but in the frontal zone. A similar partitioning of the flow was employed by Stoker for the analogous single-layer problem and has been used extensively for the analysis of compressible flow with shock waves (Courant and Friedrichs, 1976).

The equations governing the wave zone for one-dimensional, time-dependent flow are well known and given by

$$2\frac{\partial c}{\partial t} + 2u\frac{\partial c}{\partial x} + c\frac{\partial u}{\partial x} = 0 \tag{15}$$

$$\frac{\partial u}{\partial t} + u\frac{\partial u}{\partial x} + 2c\frac{\partial c}{\partial x} = 0 \tag{16}$$

where $c \equiv (g' D)^{1/2}$ is the local phase speed, (15) is the continuity equation and (16) the x-momentum equation. This system is identical in form to that of the single-layer system (Stoker, 1967, p. 292) and thus has the same two real characteristics given by $s = u \pm c$ where $s \equiv dx/dt$, the slope of the characteristic line in the x, t plane. Along the characteristic lines the dependent variables are related by the characteristic equations:

$$u + 2c = K_+ \quad \text{for } s = u + c \tag{17a}$$

$$u - 2c = K_- \quad \text{for } s = u - c \tag{17b}$$

where K_+ and K_- are constants along their respective characteristics.

The principal features of the flow appear in sketch form in Fig. 3. The upper section shows the configuration in the x, z plane at a particular time $t = \hat{t}$, while the lower shows the front and the structure of the principal characteristic lines in the x, t plane. The front is advancing toward the right at a constant velocity u_f. Beyond it the flow is still undisturbed with $D = D_0$ and $u = u_0 = 0$. On the left the upstream propagating leading wave advances at the velocity $-c_p$ into the pool where the flow is still undisturbed with $D = D_p$ and $u = u_p = 0$. Between the front and the leading wave is the wave zone. Two major regions are present there. Region I has uniform properties determined by the frontal jump conditions with $D = D_1$ and $u = u_1$. Its downstream limit is set by the front while its

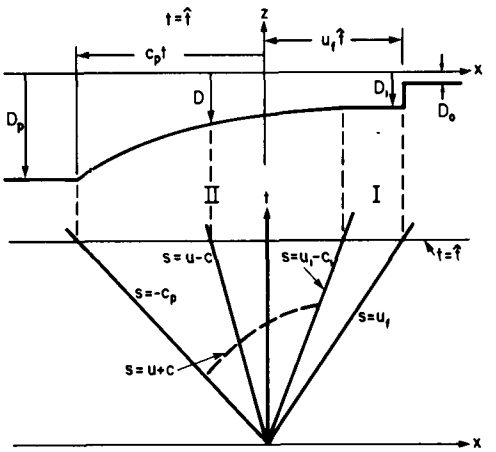

Fig. 3. Sketch of the time-dependent flow for the sudden release problem. The upper section shows the interface configuration at time $\hat{t}$ after release. The lower section shows the front and principal characteristics in the x, t plane.

upstream limit is set by the trailing upstream propagating wave whose velocity is $u_1 - c_1$. (The existence of Region I thus requires $u_f > u_1 - c_1$.) Region II spans the entire upstream propagating wave train. Since the domain of these waves is bounded on both sides by domains of uniform u and c, these waves must constitute a simple or single family wave train (Courant and Freidrichs, 1976, Chapter III). In the present case this means that along every $u + c$ characteristic, such as the one shown by the dashed line in Fig. 3, the constant K_+ of (17a) is the same. Since at the upstream limit of Region II $K_+ = 2c_p$, we have for Region II that

$$u + 2c = 2c_p \tag{18}$$

Thus, at the downstream limit we have

$$u_1 = 2(c_p - c_1) \tag{19}$$

The flow in Region I may now be determined by using (19) together with the frontal jump conditions of Section 2 specialized to the present problem. Here we have $u_a = 0$, hence $\bar{u}_a = u_f$. Since $u_0 = 0$, $\bar{u}_0 = u_f$ also. Consequently, $F_{00} = F_{a0} = u_f/c_0 \equiv F_0$ here. From (11) we may find $\delta \equiv D_1/D_0$ where now $B = 1 - 2\beta(d + S_e - \beta)F_0^2$ and $C \equiv 2(1 - S_e\beta)^2 F_0^2$. The flow behind the front in the fixed coordinates is given in terms of that seen from the frontal translating coordinates by $u_1 = u_f - \bar{u}_1$. From the frontal jump condition (12) we may write, in turn,

$$\bar{u}_1 = u_f[S_e\beta + \delta^{-1}(1 - S_e\beta)]$$

Thus, $u_1 = u_f(1 - \delta^{-1})(1 - S_e\beta)$. By combining this and (19) the following may be determined after some algebra:

$$\frac{c_p}{c_1} = 1 + \frac{F_0}{2}\delta^{-1/2}(1 - \delta^{-1})(1 - S_e\beta) \tag{20}$$

For given values of F_0, β, d and S_e, (11), (19) and (20) may be used to compute D_0, u_f and the variables in Region I. The following relations give normalized forms for these quantities.

$$D_0/D_p = \delta^{-1}(c_p/c_1)^{-2}$$

$$F_{11} \equiv u_1/c_1 = 2\left(\frac{c_p}{c_1} - 1\right)$$

$$F_{a1} \equiv u_f/c_1 = F_0\,\delta^{-1/2}$$

$$u_f/c_p = F_{a1}(c_p/c_1)^{-1}$$

A summary of the principal results appears in Figs. 4 to 7. The calculations were made for $d = 2.5$, $S_e = -1$ (downward entrainment) and β from 0 to 1 in intervals of 0.2. Downward entrainment was chosen because it is necessary for the maintenance of a mean state with respect to the mixing action of turbulence near the interface in the frontal zone and because it corresponds to the entrainment dynamics near the head wave of density currents (Britter and Simpson, 1978). The range for β includes the case of zero interfacial transport ($\beta = 0$), for which the results are identical to those of Stoker for the analogous single-layer problem, and extends to $\beta = 1$, roughly the largest expected value based on the detailed comparisons of frontal structure with field observations (G74). In each figure the abscissa is D_0/D_p, rather than F_0, since its limits are simply zero, when no upper layer is present initially for $x > 0$, and unity, when no disturbance will develop. (The corresponding limits for F_0 are ∞ and $(1 + d\beta - S_e\beta)^{-1/2}$, respectively.)

Fig. 4 shows the frontal propagation velocity u_f normalized by c_p. For any fixed D_0/D_p the velocity falls monotonically as β increases, but with changes

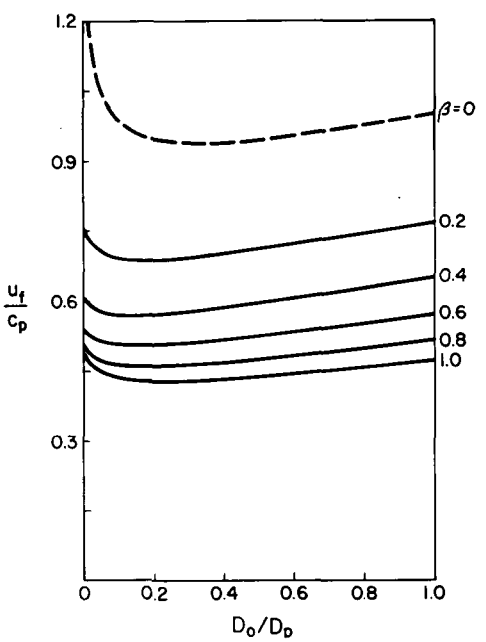

Fig. 4. Normalized frontal propagation velocity vs. D_0/D_p for six values of β from 0 to 1. The dashed line denotes $\beta = 0$.

diminishing as β approaches unity. This behavior would be expected, since increasingly positive β leads to a stronger net contribution to the momentum balance by interfacial friction and momentum entrainment [see (9)]. For $\beta \geq 0.2$, u_f/c_p is less than about 0.8 and is only weakly dependent on D_0/D_p. In contrast, for $\beta = 0$ it increases sharply to a limiting value of 2 for $D_0/D_p \to 0$. This limiting value was derived by Stoker (1957, p. 313) for the single-layer problem.

Results for the Froude number $F_{a1} = u_f/c_1$ appear in Fig. 5. For $\beta \geq 0.2$ they increase slowly with decreasing D_0/D_p and decrease slowly with increasing β. The values are not very sensitive to β, however, especially for $D_0/D_p = 0$ when all are fairly close to unity [see (14)]. This is in agreement with the numerical solutions of Kao, Park and Pao (1978, Table II) for this limit. In contrast, for small β, F_{a1} increases abruptly with declining D_0/D_p and is unbounded then for $\beta = 0$.

Fig. 6 gives an indication of the strength of the front as measured by the interfacial depth change $D_1 - D_0$ scaled by D_p. For $D_0/D_p \to 1$ no depth change occurs, since this is the limit of vanishing disturbance, irrespective of β, for which $D_0 = D_1 = D_p$, and no fluid motion results. As D_0/D_p decreases the depth change increases rapidly for all values of β (but not monotonically with β) until maximum values are reached. These maxima

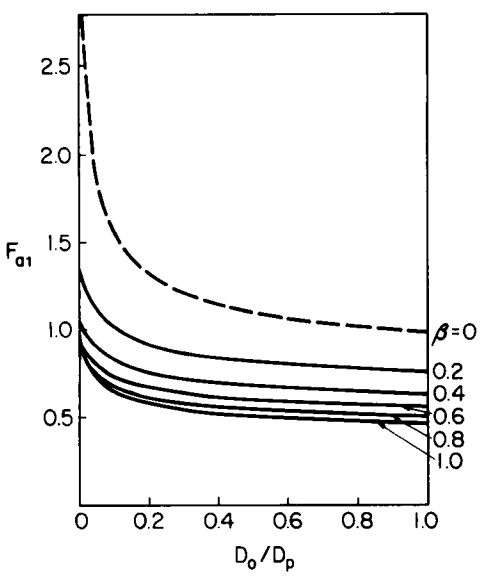

Fig. 5. Froude number $F_{a1} = u_f/c_1$ vs. D_0/D_p.

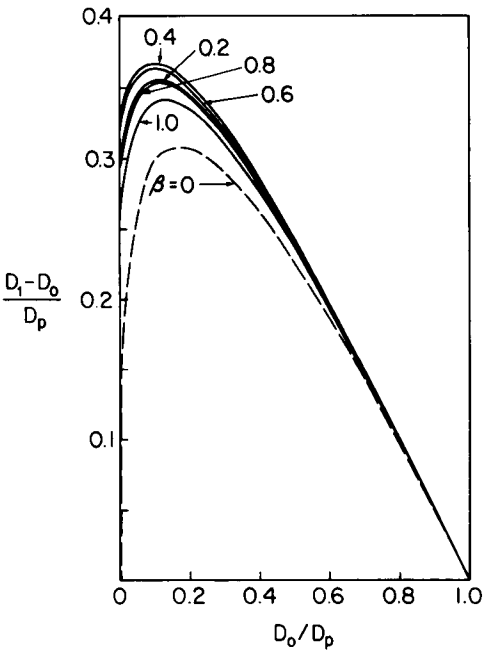

Fig. 6. Normalized interfacial depth change vs. D_0/D_p.

are equal to roughly 1/3 and are reached at D_0/D_p of roughly 0.15 with particular values depending weakly on β. For still smaller D_0/D_p the depth changes then decrease, reaching local minima at $D_0/D_p = 0$. For $\beta \geq 0.2$ these decreases are not large; however, for $\beta = 0$ the curve plunges abruptly to zero. A curve identical to that for $\beta = 0$ is given by Stoker (1957, Fig. 10.8.6) for the single-layer problem. The limiting behavior for $D_0/D_p \to 0$ when $\beta = 0$ may seem paradoxical. As D_0/D_p decreases one might expect a strong front to persist, since then the greater initial relative pool depth would seem likely to result in a toppled interface with subsequent breaking. Instead, for vanishing D_0, no front develops at all. Stoker discusses this limit in detail (pp. 311–314). The downstream limit of the advancing fluid is then a tip of zero height or cusp with velocity $2c_p$ and Region II occupies the whole of the wave zone. For positive β this physically improbable limiting behavior disappears and advancing fronts with $D_1/D_p \simeq 0.3$ are formed.

Fig. 7 shows the Froude number of Region I, $F_{11} = u_1/c_1$. For all β it vanishes as $D_0/D_p \to 1$, since u_1 vanishes then in the limit of no disturbance. For decreasing D_0/D_p it monotonically increases

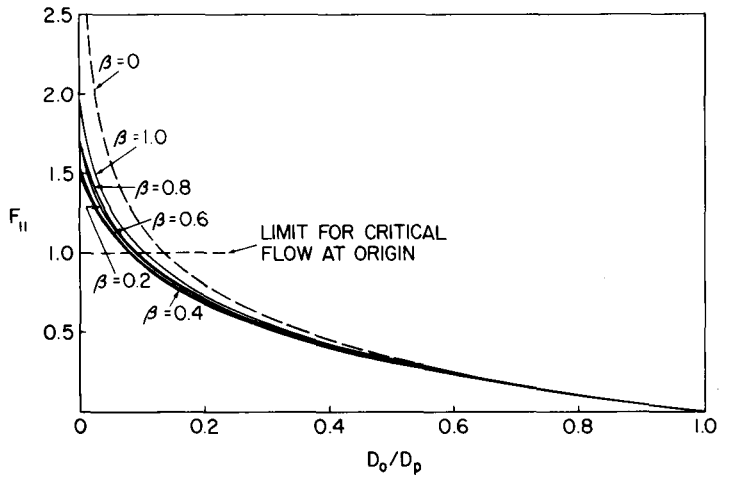

Fig. 7. Froude number $F_{11} = u_1/c_1$ vs. D_0/D_p.

for all β. Again for $\beta \geq 0.2$ the curves depend only weakly on β and, as for the depth change, this dependence is not monotonic. For vanishing D_0 these curves have maxima for F_{11} in the range of 1.5 to 1.9. If we compare these values to those for F_{a1} in Fig. 5 for $D_0/D_p = 0$, we deduce that then $u_1 > u_f$, i.e., that the fluid behind the front is overtaking it, or that the front is a region of horizontal convergence. This behavior arises from the specification of downward entrainment in the frontal zone ($S_e = -1$) and is consistent with the numerical results of Kao, Park and Pao (1977) and the observations of Garvine and Monk (1974).

A dashed line in Fig. 7 indicates the critical flow point ($F_{11} = 1$) where it intersects each curve. For smaller values of D_0/D_p on a given curve the flow in Region I will be supercritical; hence, the flow at the origin (the dam site in the single-layer problem) will be supercritical also, and thus the origin could then serve as a hydraulic control point. Any changes imposed there on the flow, such as a change in depth, would produce waves which would be swept downstream, and no flow changes downstream could subsequently alter the flow at the origin. Larger values of D_0/D_p correspond to subcritical flow. The origin could not then serve as a control and the upstream limit of Region I will then propagate upstream, in contrast to the sketch of Fig. 3. Thus, for $F_{11} \geq 1$ the flow at the origin will remain independent of all flow properties downstream, including D_0, while for $F_{11} < 1$, it will depend on the downstream flow, including D_0. For $\beta = 0$ the critical value of D_0/D_p is 0.1384, as Stoker found, while for $\beta \geq 0.2$ the critical values are lower at roughly 0.09.

The results for Region I variables permit an assessment of the condition for the existence of the region given above as $u_f > u_1 - c_1$. This may be restated in normalized form as $F_{a1} > F_{11} - 1$. As may be verified from Figs. 5 and 7, this condition is always satisfied for all β for the present results.

The flow structure of Region II is readily found. Each of the u-c characteristics is straight and originates at the origin (Fig. 3). Thus, $dx/dt = x/t = u$-c. Then, from (18) c and u may be expressed in dimensionless form as,

$$\frac{c}{c_p} = \frac{1}{3}\left(2 - \frac{x}{c_p t}\right) \tag{21a}$$

$$\frac{u}{c_p} = \frac{2}{3}\left(1 + \frac{x}{c_p t}\right) \tag{21b}$$

The shape of the interface is then determined simply by $D/D_p = (c/c_p)^2 = (2 - x/c_p t)^2/9$, a parabola. The upstream limit of Region II is at $x/c_p t = -1$ where $D = D_p$, while the downstream limit is at $x/c_p t = (u_1 - c_1)/c_p = (F_{11} - 1)c_1/c_p$. Thus, for $F_{11} \geq 1$, the origin ($x = 0$) is within Region II. Then, from (21) we find that there $u = c = 2c_p/3$ for all $t > 0$. Consequently, the local Froude number is then always critical with the flow upstream subcritical. Furthermore, at the origin $D/D_p = 4/9$ and the volume flux is fixed at

$uD = (8/27)c_p D_p$. These results for $F_{11} \geq 1$ are identical to Stoker's for the single-layer problem, since only the downstream limit of Region II depends upon the results of Region I which depend, in turn, upon β.

4. Concluding remarks

The frontal jump conditions derived in this paper make possible a simplified description of the hydrodynamics of buoyant, shallow surface layers when used as boundary conditions for the long, nonlinear internal wave equations. The degree to which this description is accurate remains to be determined. This will require both that computations for a variety of problems be completed and and that these be compared with relevant field observations and laboratory studies.

The jump conditions could be extended to include the influence of earth rotation and surface wind stress by following the conceptual frame used in extending the frontal integral model of G74 to that including these effects, as described in Garvine (1979). Without major alteration the jump conditions derived here could be applied also to the problem of density currents spreading over a solid, level surface, provided that bottom stress were neglected. Still other potential applications may appear as we learn more of the hydrodynamics of coastal and inland waters.

5. Acknowledgement

This study was supported by the National Science Foundation under Grant No. OCE-7821318.

REFERENCES

Britter, R. E. and Simpson, J. E. 1978. Experiments on the dynamics of a gravity current head. *J. Fluid Mech. 88*, 223–240.

Courant, R. and Friedrichs, K. O. 1976. *Supersonic flow and shock waves*. New York: Interscience Publishers, Inc.

Garvine, R. W. 1974a. Physical features of the Connecticut River outflow during high discharge. *J. Geophys. Res. 79*, 831–846.

Garvine, R. W. 1974b. Dynamics of small-scale oceanic fronts. *J. Phys. Oceanogr. 4*, 557–569.

Garvine, R. W. 1977. Observations of the motion field of the Connecticut River plume. *J. Geophys. Res. 82*, 441–454.

Garvine, R. W. 1979. An integral, hydrodynamic model of upper ocean frontal dynamics: Part I. Development and analysis. *J. Phys. Oceanogr. 9*, 1–18.

Garvine, R. W. and Monk, J. D. 1974. Frontal structure of a river plume. *J. Geophys. Res. 79*, 2251–2259.

Grancini, G. and Cescon, B. 1973. Dispersal processes of freshwater in the Po River coastal area. *Limnol. and Oceanogr. 9*, 467–475.

Hunkins, K. and Fliegel, M. 1973. Internal undular surges in Seneca Lake: A natural occurrence of solitons. *J. Geophys. Res. 78*, 539–548.

Kao, T. W., Park, C. and Pao, H.-P. 1977. Buoyant surface discharge and small-scale oceanic fronts: a numerical study. *J. Geophys. Res. 82*, 1747–1766.

Kao, T. W., Park, C. and Pao, H.-P. 1978. Inflows, density currents, and fronts. *Phys. Fluids. 21*, 1912–1922.

Mehrotra, S. C. 1973. Limitations on the existence of shock solutions in a two-fluid system. *Tellus 25*, 169–173.

Mehrotra, S. C. and Kelly, R. E. 1973. On the question of non-uniqueness of internal hydraulic jumps and drops in a two-fluid system. *Tellus 25*, 560–567.

Ryther, J. H., Menzel, D. W. and Corwin, N. 1967. Influence of the Amazon River outflow on the ecology of the western tropical Atlantic, 1, Hydrography and nutrient chemistry. *J. Mar. Res. 25*, 69–83.

Scarpace, F. L. and Green, T. III. 1973. Dynamic surface temperature structure of thermal plumes. *Water Resources Res. 9*, 138–153.

Simons, T. J. 1978. Generation and propagation of downwelling fronts. *J. Phys. Oceanogr. 8*, 571–581.

Stefan, H. and Vaidyaraman, P. 1972. Jet type model for the three-dimensional thermal plume in a cross-current and under wind. *Water Resources Res. 8*, 998–1014.

Stoker, J. J. 1957. *Water waves*. New York: Interscience Publishers, Inc.

Takano, K. 1954. On the salinity and velocity distribution off the mouth of a river. *J. Oceanogr. Soc. Japan 10*, 92–98.

Von Kármán, T. 1940. The engineer grapples with nonlinear problems. *Bull. Amer. Math. Soc. 46*, 615–683.

Wright, L. D. and Coleman, J. M. 1971. Effluent expansion and interfacial mixing in the presence of a salt wedge, Mississippi River Delta. *J. Geophys. Res. 76*, 8649–8661.

Yih, C.-S. and Guha, C. R. 1955. Hydraulic jump in a fluid system of two layers. *Tellus 7*, 358–366.

УСЛОВИЯ НА ФРОНТАЛЬНОМ СКАЧКЕ ДЛЯ МОДЕЛЕЙ ГИДРОДИНАМИКИ МЕЛКОГО ПОВЕРХНОСТНОГО СЛОЯ С ПЛАВУЧЕСТЬЮ

В прибрежных и внутренних водах в присутствии поверхностного слоя с плавучестью часто наблюдаются движущиеся фронтальные области. Примерами таких явлений служат движущиеся фронты, позади которых происходит растекание плавучих поверхностных языков и прохождение выхода термоклина на поверхность в озерах. Предлагается подход к моделированию гидродинамики мелких поверхностных слоев с плавучестью, где поле течений разделяется на фронтальную область, в которой важны эффекты диссипации, и область внутренних волн, где диссипация мала. В этом подходе фронтальная область рассматривается как горизонтальный разрыв, описываемый соответствующими условиями на скачке, а для волновой области используются нелинейные уравнения для длинных внутренних волн. В применении к мелкомасштабным течениям, когда можно пренебречь вращением Земли, выводятся условия скачка на фронте. Эти условия учитывают перенос массы и импульса через поверхность раздела с нижележащей жидкостью. Они так же применимы к потокам, где глубина верхнего плавучего слоя исчезает на стороне фронта вверх по течению. Таким образом, они представляют собой обобщение классических условий на скачках, связанных с внутренним бором или с гидравлическим скачком. Для иллюстрации их использования совместно с нелинейными уравнениями для внутренних волн решается задача о внезапном напуске мелкого верхнего плавучего слоя в неограниченную область. Для нулевого переноса через поверхность раздела результаты идентичны классическому описанию аналогичной задачи о слое, вводимом внезапным разрушением плотины. Однако для ненулевого переноса возникают новые особенности в поле течений.